Published in final edited form as:

Hepatology. 2015 June ; 61(6): 1887–1895. doi:10.1002/hep.27666.

Magnetic Resonance Imaging and Liver Histology as Biomarkers of Hepatic Steatosis in Children with Nonalcoholic Fatty Liver Disease

Jeffrey B. Schwimmer, M.D.[1,2,3], **Michael S. Middleton, M.D., Ph.D.**[3], **Cynthia Behling, M.D., Ph.D.**[1,4], **Kimberly P. Newton, M.D.**[1,2], **Hannah I. Awai, M.D.**[1,2,3], **Melissa N. Paiz, B.S.**[1], **Jessica Lam, B.S.**[3,5], **Jonathan C. Hooker, B.S.**[3], **Gavin Hamilton, Ph.D.**[3], **John Fontanesi, Ph.D.**[6,7,8], and **Claude B. Sirlin, M.D.**[3]

Jeffrey B. Schwimmer: jschwimmer@ucsd.edu; Michael S. Middleton: msm@ucsd.edu; Cynthia Behling: Cynthia.Behling@sharp.com; Kimberly P. Newton: kpnewton@ucsd.edu; Hannah I. Awai: hawai@ucsd.edu; Melissa N. Paiz: mpaiz@ucsd.edu; Jessica Lam: jelam@llu.edu; Jonathan C. Hooker: jhooker@ucsd.edu; Gavin Hamilton: ghamilton@ucsd.edu; John Fontanesi: jfontanesi@ucsd.edu; Claude B. Sirlin: csirlin@ucsd.edu

[1]Division of Gastroenterology, Hepatology, and Nutrition, Department of Pediatrics, University of California, San Diego School of Medicine, San Diego, California

[2]Department of Gastroenterology, Rady Children's Hospital San Diego, San Diego, California

[3]Liver Imaging Group, Department of Radiology, University of California, San Diego School of Medicine, San Diego, California

[4]Department of Pathology, Sharp Medical Center, San Diego, California

[5]School of Medicine, Loma Linda University, Loma Linda, California

[6]Center for Management Science in Health, Division of General Internal Medicine, Department of Medicine, University of California, San Diego School of Medicine, La Jolla, California

[7]Department of Family and Preventive Medicine, University of California, San Diego School of Medicine, La Jolla, California

[8]Department of Pediatrics, University of California, San Diego School of Medicine, La Jolla, California

Abstract

Nonalcoholic fatty liver disease (NAFLD) is the most common chronic liver disease in children. In order to advance the field of NAFLD, noninvasive imaging methods for measuring liver fat are needed. Advanced magnetic resonance imaging (MRI) has shown great promise for the quantitative assessment of hepatic steatosis but has not been validated in children. Therefore, this study was designed to evaluate the correlation and diagnostic accuracy of MRI-estimated liver proton density fat fraction (PDFF), a biomarker for hepatic steatosis, compared to histologic steatosis grade in children. The study included 174 children with a mean age of 14.0 years. MRI-estimated liver PDFF was significantly ($p < 0.01$) correlated (0.725) with steatosis grade.

Correspondence: Jeffrey B. Schwimmer, M.D., Division of Gastroenterology, Hepatology, and Nutrition, Department of Pediatrics, University of California, San Diego, 3020 Children's Way, MC 5030 San Diego, CA 92123, jschwimmer@ucsd.edu, phone: 858-966-8907, fax: 858-560-6798.

Correlation of MRI-estimated liver PDFF and steatosis grade was influenced by both sex and fibrosis stage. The correlation was significantly ($p<0.01$) stronger in girls (0.86) than in boys (0.70). The correlation was significantly ($p<0.01$) weaker in children with stage 2–4 fibrosis (0.61) than children with no fibrosis (0.76) or stage 1 fibrosis (0.78). The diagnostic accuracy of commonly used threshold values to distinguish between no steatosis and mild steatosis ranged from 0.69 to 0.82. The overall accuracy of predicting the histologic steatosis grade from MRI-estimated liver PDFF was 56%. No single threshold had sufficient sensitivity and specificity to be considered diagnostic for an individual child.

Conclusions—Advanced magnitude-based MRI can be used to estimate liver PDFF in children, and those PDFF values correlate well with steatosis grade by liver histology. Thus magnitude-based MRI has the potential for clinical utility in the evaluation of NAFLD, but at this time no single threshold value has sufficient accuracy to be considered diagnostic for an individual child.

Keywords

Proton density fat fraction; liver biopsy; obesity; pediatrics; fibrosis

INTRODUCTION

Nonalcoholic fatty liver disease (NAFLD) is the most common chronic liver disease in children(1). NAFLD may progress to cirrhosis and hepatocellular carcinoma(2, 3), and is associated with diabetes(4–6) and cardiovascular disease(4, 7, 8). The clinical reference standard for diagnosis of NAFLD is liver biopsy with interpretation of histology by a pathologist(9–11). Although liver biopsy is valuable in many settings, the requirement for liver biopsy to evaluate NAFLD hampers clinical care and impedes research.

In order to advance the field of NAFLD, noninvasive imaging methods for measuring liver fat are needed. Although ultrasound is widely used as a non-invasive tool to assess NAFLD, it has limited sensitivity and specificity(12). Magnetic resonance imaging (MRI) has shown greater promise for the quantitative assessment of hepatic steatosis. In adults, reported correlations between MRI-estimated measures of liver fat and histologic steatosis grade have ranged from moderate to strong(13–19); however, there is insufficient data to be able to translate estimates of liver fat content by MRI directly into a specific steatosis grade. In addition, data are mixed regarding whether or not the relationship is influenced by factors such as hepatic fibrosis stage(13, 15, 20–23). Moreover, data generated in adults cannot be directly applied to the pediatric population. Children differ from adults in several key aspects including body habitus, breath-hold capacity, and ability to tolerate imaging examinations. These factors can affect the feasibility, quality, and technical optimization of imaging examinations and may affect their diagnostic performance. Currently, data in children are extremely limited.

The MRI Rosetta Stone Project was based upon a desire to understand in children the meaning of a given value of liver proton density fat fraction (PDFF), an MRI-based biomarker of liver fat content, in the context of liver fat as measured by liver histology. This study had the following aims:

1. To determine the correlation between MRI-estimated liver PDFF and histologic steatosis grade and to test for effect modification by age, sex, and fibrosis stage.
2. To test the accuracy of MRI-estimated liver PDFF in predicting histologic steatosis grade.
3. To test proposed threshold scores for MRI-estimated liver PDFF to discriminate between children with a histologic steatosis grade of 0 (no steatosis) and a histologic steatosis grade of 1 (mild steatosis). The ability of a non-invasive test to accurately classify a child as having or not having fatty liver is based upon both the ability of that test to separate between histologic grades 0 and 1, and the distribution of liver fat within the test population. For this study we chose to focus on this separation between grade 0 and grade 1 because this is more specific to the test itself, rather than the population in which it is being applied.

METHODS

Study design

We included children ages 8 to 17 years in a prospective study to evaluate the stated aims. All children had already undergone liver biopsy as part of a clinical evaluation for liver disease. The determination to perform liver biopsy was done clinically and was not part of this study. The parent(s) or legal guardian of all subjects provided written informed consent. Written assent was obtained from all children. The protocol was approved by the institutional review boards of the University of California, San Diego and Rady Children's Hospital San Diego.

Subject selection

Controls—In order to address the study aims we included children who had liver biopsies that showed no steatosis as well as children with biopsy-proven NAFLD. Children without steatosis were a convenience sample of children who already had liver biopsy performed and were known to have normal histology or had a diagnosis of liver disease that did not involve steatosis.

NAFLD—The diagnosis of NAFLD was based on exclusion of other causes of steatosis by clinical history, laboratory studies, and histology in addition to histologic demonstration of ≥ 5% of hepatocytes containing macrovesicular fat(24). The study was designed to include equal numbers of children with NAFLD in each of the three steatosis grades: mild, moderate, and severe. We recruited consecutive children with NAFLD meeting eligibility until each category achieved the target goal of 50 subjects.

Clinical data collection

Clinical data were obtained for each participant at a single fasting intake visit conducted at the Clinical and Translational Research Institute at the University of California, San Diego Medical Center. Each participant's age and gender were recorded. Height was measured to the nearest tenth of a centimeter on a clinical stadiometer. Weight was measured on a clinical scale to the nearest tenth of a kilogram. Body mass index (BMI) was calculated as

weight in kilograms divided by height in meters squared. Phlebotomy was performed after a 12-hour overnight fast, and assays for serum alanine aminotransferase (ALT), aspartate aminotransferase (AST) and gamma-glutamyl transferase (GGT) were performed using an enzymatic rate method.

Histopathology

Slides were reviewed by a hepatopathologist utilizing the Nonalcoholic Steatohepatitis Clinical Research Network scoring system(25). The amount of surface area of parenchyma involved by steatosis was determined at low power. Steatosis was graded according to the percentage of hepatocytes that contained fat droplets as follows: grade 0, none: < 5%; grade 1, mild: 5 to 33%; grade 2, moderate: 34 to 66%; and grade 3, severe: > 66%. Fibrosis was staged as follows: a) stage 1a – mild zone 3 perisinusoidal fibrosis requiring trichrome stain; b) stage 1b – moderate zone 3 perisinusoidal fibrosis not requiring trichrome stain; c) stage 1c -- portal/periportal fibrosis only; c) stage 2 --zone 3 perisinusoidal fibrosis and periportal fibrosis; d) stage 3 -- bridging fibrosis; and e) stage 4 -- cirrhosis.

MRI acquisition protocol

Children were scanned at 3T using an advanced magnitude-based liver fat quantification MRI technique. This gradient-recalled-echo technique estimates liver PDFF using low flip angle and repetition time (TR) of ≥ 150 msec to minimize T_1 bias(26, 27), and six gradient-recalled echoes to calculate and correct for T_2* signal decay(26, 28, 29).

MRI analysis

MRI-estimated liver PDFF parametric maps were computed pixel-by-pixel from source images using custom-developed software that models observed signal as a function of echo time (TE), taking into account the multiple frequency components of triglyceride. PDFF values were obtained by placing regions of interest (ROIs) in representative portions of the liver on those maps. Because percutaneous liver biopsy samples the right lobe of the liver, we restricted the MRI evaluation to the right lobe; PDFF values in ROIs placed in each of the four right-lobe segments were averaged to provide a composite right lobe MRI-estimated PDFF value.

Blinding

The MR technologist performing the MRI scan and the image analyst placing the ROIs on the liver PDFF parametric maps were unaware of steatosis grade results. Similarly the pathologist was not aware of MRI results.

Data analysis

Data were expressed as mean ± standard deviation (if not normally distributed then geometric means were reported) or frequency and percentage. Initial data exploration of continuous variables used Student's t test with Mann–Whitney U test for nonparametric measures and Pearson Chi-Square test to test for differences in proportions. All hypothesis tests were 2-tailed. Significance was defined *a priori* at α value of 0.05. Analyses were performed with Statistica 10 (StatSoft, Inc., Tulsa, OK).

In aim 1, we evaluated the correlation between MRI-estimated liver PDFF and histologic steatosis grade (an ordinal variable) using GAMMA correlation(30). We tested for effect modification by age, sex and fibrosis stage using Fisher r-to-z transformation and Steiger's Z-test for multiple correlations. In aim 2, we used ordinal multinomial logit to measure the probability of any given MRI-estimated liver PDFF value corresponding to a steatosis grade of 0, 1, 2, or 3. Cross-validation and resampling were used to quantify the bias-variance tradeoff for contextual factors explored in aim 1. For illustration purposes only, we calculated probabilities of specific representative MRI-estimated PDFF values corresponding to specific steatosis grades. The overall accuracy of the probabilistic model was determined and the corresponding odds ratio was calculated. Finally, in aim 3, we assessed the sensitivity and specificity for each of 4 published MR-derived threshold values (1.8%, 5.5%, 6.4%, and 9.0%) intended to discriminate between steatosis grade 0 and grade 1. From these, receiver operating characteristic (ROC) curves were generated and areas under the ROC curves were calculated.

We performed a post-hoc analysis to derive and test the optimal cut-point to separate between no steatosis and any steatosis (mild, moderate, or severe) for the Rosetta Stone data set presented in this manuscript. Because of the potential for over-fitting that occurs when a threshold is tested in the same population in which it was derived, we also tested the cut-point along with the existing published cut-points via simulations using data from 2 prior pediatric studies with histology(1, 31). Due to space constraints, full details about these methodologies along with the results of the post-hoc analyses are available in an online supplement.

RESULTS

Study population

The MRI Rosetta Stone Project included 174 children with a mean age of 14.0 years. The demographics and clinical features of the participants separated by steatosis grade are shown in Table 1. The ordinal severity of steatosis across the four grades was significantly positively associated with serum ALT, AST, and GGT. The distribution of fibrosis severity was stage 0: 57% (99/174), stage 1: 25.8% (45/174), stage 2: 2.3% (4/174), stage 3: 11.5% (20/174), and stage 4: 3.4% (6/174).

Aims 1: Correlation between MRI and steatosis

An example of MRI-estimated liver PDFF parametric maps is shown for each steatosis grade in Figure 1. The mean time interval between MRI and liver biopsy was 57 ± 51 days and was not significantly different across the different grades of steatosis ($p = 0.97$). All children were able to complete the MRI acquisition protocol without difficulty. The mean value for MRI-estimated liver PDFF by steatosis grade was 2.6% for grade 0, 9.2% for grade 1, 15.1% for grade 2, and 26.8% for grade 3. MRI-estimated liver PDFF was significantly ($p < 0.01$) correlated (0.725) with the histologically-determined steatosis grade. The distribution of MRI-estimated liver PDFF by steatosis grade is shown in Figure 2. The correlation of MRI-estimated liver PDFF and steatosis grade was not influenced by age as a continuous or categorical variable. In contrast, the correlation of MRI-estimated liver PDFF

and steatosis grade was influenced by both sex and fibrosis stage. The correlation was significantly ($Z = -2.57$, $p<0.01$) stronger in girls (0.86) than in boys (0.70). The correlation was significantly ($Z = -4.31$, $p<0.001$) weaker in children with stage 2–4 fibrosis (0.61) than children with no fibrosis (0.76) or stage 1 fibrosis (0.78).

Aim 2: Probability predictions for steatosis score

Figure 3 shows a heat map for the probability of any given MRI-estimated liver PDFF value corresponding to a steatosis grade of 0, 1, 2, or 3. The prediction probabilities are strongest at the low and high ends of the PDFF range, as illustrated by three representative examples. On the low end of the PDFF spectrum, a child with a PDFF of 2% has a probability of 95% for steatosis grade 0, 5% for steatosis grade 1, and 0% for steatosis grade 2 or 3. On the high end of the PDFF spectrum, a child with a PDFF of 30 has a probability of 0% for steatosis grade 0 or 1, 5% for steatosis grade 2, and 95% for steatosis grade 3. However in the midrange, a child with a PDFF of 15 has a probability of 0% for steatosis grade 0, 19% for steatosis grade 1, 68% for steatosis grade 2, and 13% for steatosis grade 3. The overall accuracy of ordinal multinomial logit to predict the histologically-determined steatosis grade from MRI-estimated liver PDFF was 56% (95% CI = 54 – 60%); odds ratio 3.27 (95% CI = 3.17–3.41).

Aim 3: Diagnostic accuracy to distinguish between steatosis grade 0 and grade 1

We tested the diagnostic accuracy of published potential threshold values to distinguish between no steatosis and mild steatosis (Table 2). The sensitivity ranged from 42 to 98 percent while the specificity ranged from 54 to 96 percent. The ROC curves are shown in Figure 4. The AUROC was significant ($p<0.001$) for all 4 published cut-points.

We identified the optimal cut-point for the separation of no steatosis from any degree of steatosis (mild, moderate, or severe) in the Rosetta Stone study sample. We then applied this threshold along with the previously published thresholds to the Rosetta Stone study sample as well as simulating the performance in two real world data sets. In the general population and in children with suspected NAFLD. These data demonstrate the impact of the distribution of disease on the diagnostic utility of any given cut-point.

DISCUSSION

We performed a large study of children with and without NAFLD that included both liver histology and advanced magnitude-based liver MRI. MRI was well-tolerated with quality data produced in all children. MRI-estimated liver PDFF was shown to be strongly correlated with the histologic steatosis grade. This correlation was influenced by both sex and fibrosis stage. Published thresholds to separate normal liver from mild steatosis varied widely in their ability to discriminate between grade 0 and grade 1 steatosis. These data advance the understanding of the non-invasive measurement of hepatic steatosis in children using MRI.

The correlation observed in our study between MRI-estimated liver PDFF and histologic steatosis grade was in the low end of the range of published correlations. In adults, those correlations have ranged from 0.68 to 0.91(13, 17–19). In prior pediatric studies, there was a

correlation between MRI-estimated liver fat and steatosis grade of 0.88 – 0.90. However, these studies had small sample sizes with a total of 10 to 25 cases with histology and controls with no histology(32, 33). In general, the highest correlations have been found in studies with the smallest population sample sizes and/or with the greatest skew. For example, Hatta et al found a correlation of 0.91 in a study of 26 adults with NAFLD(34) and Lee et al found a correlation of 0.84 in study of potential liver donors in which 63% of patients had a steatosis grade of 0(35). In contrast, those studies that had larger sample sizes and/or more heterogeneous populations found lower correlations. For example, Tang et al found a correlation of 0.69 in a study of 77 subjects with NAFLD(13) and Qayyum et al found a correlation of 0.68 in a study of subjects with NAFLD, Hepatitis C virus, or other chronic liver disease(19). Moreover, in order to understand the limits of best achievable correlation between histologic and MR-based measures of steatosis, it is important to consider how steatosis is estimated by these different methods.

The histologic grading of steatosis is done by a pathologist visually estimating the fraction of hepatocytes that contain lipid droplets. Grading is done using a semi-quantitative ordinal scoring system with four broad brackets of steatosis severity. Of the boundaries created in grading hepatic steatosis, the most important one is the separation between histologic grades 0 (no steatosis) and 1 (mild steatosis). This distinction determines whether or not a child is considered to have fatty liver. Since the actual amount of steatosis is a continuous variable, grading steatosis in a four-point ordinal scale introduces potential misclassification of steatosis severity at the boundaries created between grades. The estimation also does not take into account factors that influence the amount of fat present such as the size of the lipid droplets.

In contrast, MR-based methods can be used to measure liver fat as a continuous variable; MR spectroscopy or MR imaging assess hepatic fat by estimating either the signal fat fraction (SFF) or the proton density fat fraction (PDFF)(36). The signal fat fraction (SFF) is the proportion of the MR signal that comes from fat. Since the fat signal depends not only on the underlying fat content but also on numerous confounding variables, the SFF may not reliably reflect actual fat content. Moreover, the SFF is technique and scanner dependent. The PDFF is the SFF after all major confounding effects are removed and thus reflects the actual fat content(37). It is also technique and scanner independent. Studies have shown that PDFF estimated by MR spectroscopy and MR imaging agree closely with one another(20, 22, 38) and that PDFF correlates with tissue triglyceride concentration(28, 29, 37, 39–41). Therefore the choice of MR methodology has influenced prior studies that have proposed MR-based cutoff points to allow dichotomous separation of steatosis grades 0 and 1.

The lowest cutoff point values were obtained in studies that used MR spectroscopy to estimate liver SFF. Van Werven et al proposed a cutoff point based upon PRESS MR spectroscopy of 1.8% in a study of 46 adults undergoing liver resection for liver mass; one half of whom had no histologic steatosis(42). In the Dallas Heart Study, the threshold for normal liver fat content was determined by PRESS MR spectroscopy to be 5.5% in 345 adults age 30–65 with BMI < 25 and normal labs, but no liver biopsy(43). A mid-range cutoff value was found in a study from the NASH Clinical Research Network using magnitude-based MRI-estimated liver PDFF that proposed a threshold of 6.4% based upon a

mixed population of adults and children that included five subjects with grade 0 steatosis and 26 subjects with grade 1 steatosis(13). The highest value proposed, 9%, was derived in a study of the statistical distribution of hepatic steatosis in 28 healthy medical students using two-point Dixon MRI measure of SFF and no liver biopsy(44). Each of these cutoff point values have been subsequently used by many authors to classify subjects and/or patients as having or not having fatty liver. However, the current study demonstrates that achieving a clean separation between not having fatty liver (steatosis grade 0) and having fatty liver (steatosis grade 1) based upon a single MR-based cutoff point remains challenging. Thus, it may be appropriate to include an indeterminate group, and the size of this group will depend upon the rate of classification error that one is willing to accept. Such a decision would likely be different for an epidemiology study based upon groups than it would be in clinical practice for the individual patient.

Because most of what is known about the clinical phenotype and natural history of NAFLD is based upon histology, it is important to calibrate MRI-estimated liver PDFF to what is already known about liver histology in NAFLD. Prediction of histologic steatosis grade from MRI-estimated liver PDFF was novel. We used data from this study to generate probabilities that a given MRI-estimated liver PDFF would represent a given steatosis grade rather than trying to stipulate one specific grade for any single measurement. Such an approach is a vital step in the transition of MRI as a tool for the individual rather than only for use in group studies. In addition, the ability to interpret the meaning of a given MRI-estimated liver PDFF value is essential for the application of MRI as a meaningful longitudinal tool. As is true for most biomarkers, performance was best in the highest and lowest groups, with the greatest amount of noise in the middle. A priority for future studies should be to improve diagnostic accuracy in the mild to moderate range of steatosis.

In our study we found that the relationship between MRI-estimated liver PDFF and the histologic steatosis grade was influenced by the fibrosis stage, which contributes to the challenge of direct translation between the two diagnostic modalities. The data on effect modification by fibrosis can be interpreted in the context of the above discussion along with details of the existing literature. In the setting of substantial fibrosis, there will be fewer hepatocytes per slide, however, the pathologist still reports the percentage of hepatocytes with steatosis. Thus, fibrosis may lead to a reduction in the actual percentage of the liver comprised of fat which could be reflected by the MRI-estimated PDFF value to a greater extent than it would by histological evaluation. Therefore, one should expect for fibrosis to influence the correlation between estimates made by MRI and histology. Papers that reported that fibrosis stage was not a confounding factor tended to have smaller sample sizes (13, 15, 21). Also the higher the percentage of participants with advanced fibrosis, the more likely that effect modification by fibrosis would be reported. The studies that reported no effect of fibrosis stage had only 0–10% of participants with advanced fibrosis (13, 15, 21), whereas those studies that did show an effect of fibrosis stage had 15–25% of participants with advanced fibrosis(20, 22, 23). For this reason, MR-based modalities to estimate fibrosis such as elastography may be useful to improve the ability to predict histologic steatosis grade non-invasively in the future.

The current study was notable for the large sample size of well-characterized children. Children had liver histology evaluated in a standardized fashion by an expert liver pathologist. We used an advanced magnitude-based MRI technique at 3T that acquires gradient-echo images of the liver using low flip angle to minimize T1 bias, multiple echoes to correct for T2* decay, and a multi-peak spectral model to address the multi-frequency signal interference effects of protons in fat. Because liver biopsy and MR imaging were not done on the same day, the time interval between studies may have introduced an unknown degree of error in the assessment of correlation. In addition, despite the large sample size for this type of study, there is a need for further data on even larger numbers to refine the interpretation of the relationship between MR imaging-estimated PDFF and liver histology in children. For example, one important question will be to determine if the stronger correlation observed in girls than boys was due to the smaller number of girls in this study or whether it is due to a fundamental biological difference.

Conclusion

In the MRI Rosetta Stone Project we demonstrated that magnitude-based MRI of the liver can be used to estimate PDFF in children, and those PDFF values correlate well with hepatic steatosis assessed by liver histology. Thus MRI has sufficient potential to have clinical utility in the evaluation of NAFLD. However, MRI is not yet sufficient to replace liver biopsy in children. How to best integrate MRI into clinical protocols and whether MR-based techniques such as MR elastography may be synergistic with MRI-estimated liver PDFF for the assessment of NAFLD need to be prospectively evaluated.

Supplementary Material

Refer to Web version on PubMed Central for supplementary material.

Acknowledgments

Funding: This work was supported in part by UL1RR031980 from the NCRR for the Clinical and Translational Research Institute at UCSD, DK088925-02S1, R56-DK090350-01A1, and NSF GRANT #414916. The funders did not participate in the design and conduct of the study; collection, management, analysis, and interpretation of the data; and preparation, review, or approval of the manuscript. The contents of this work are solely the responsibility of the authors and do not necessarily represent the official views of the National Institutes of Health or the National Science Foundation.

Abbreviations

NAFLD	nonalcoholic fatty liver disease
MRI	magnetic resonance imaging
PDFF	proton density fat fraction
ALT	alanine aminotransferase
AST	aspartate aminotransferase
GGT	gamma glutamyltransferase
SFF	signal fat fraction

PRESS	point resolved spectroscopy
STEAM	stimulated echo acquisition mode

References

1. Schwimmer JB, Deutsch R, Kahen T, Lavine JE, Stanley C, Behling C. Prevalence of fatty liver in children and adolescents. Pediatrics. 2006; 118:1388–1393. [PubMed: 17015527]
2. Feldstein AE, Charatcharoenwitthaya P, Treeprasertsuk S, Benson JT, Enders FB, Angulo P. The natural history of non-alcoholic fatty liver disease in children: a follow-up study for up to 20 years. Gut. 2009; 58:1538–1544. [PubMed: 19625277]
3. Alexander J, Torbenson M, Wu TT, Yeh MM. Non-alcoholic fatty liver disease contributes to hepatocarcinogenesis in non-cirrhotic liver: a clinical and pathological study. J Gastroenterol Hepatol. 2013; 28:848–854. [PubMed: 23302015]
4. Schwimmer JB, Pardee PE, Lavine JE, Blumkin AK, Cook S. Cardiovascular risk factors and the metabolic syndrome in pediatric nonalcoholic fatty liver disease. Circulation. 2008; 118:277–283. [PubMed: 18591439]
5. Rubinstein E, Lavine JE, Schwimmer JB. Hepatic, cardiovascular, and endocrine outcomes of the histological subphenotypes of nonalcoholic fatty liver disease. Semin Liver Dis. 2008; 28:380–385. [PubMed: 18956294]
6. Ekstedt M, Franzen LE, Mathiesen UL, Thorelius L, Holmqvist M, Bodemar G, Kechagias S. Long-term follow-up of patients with NAFLD and elevated liver enzymes. Hepatology. 2006; 44:865–873. [PubMed: 17006923]
7. Sanches PL, de Piano A, Campos RM, Carnier J, de Mello MT, Elias N, Fonseca FA, et al. Association of nonalcoholic fatty liver disease with cardiovascular risk factors in obese adolescents: The role of interdisciplinary therapy. J Clin Lipidol. 2014; 8:265–272. [PubMed: 24793347]
8. Kim NH, Park J, Kim SH, Kim YH, Kim DH, Cho GY, Baik I, et al. Non-alcoholic fatty liver disease, metabolic syndrome and subclinical cardiovascular changes in the general population. Heart. 2014
9. Schwimmer JB, Behling C, Newbury R, Deutsch R, Nievergelt C, Schork NJ, Lavine JE. Histopathology of pediatric nonalcoholic fatty liver disease. Hepatology. 2005; 42:641–649. [PubMed: 16116629]
10. Brunt EM. Nonalcoholic steatohepatitis: definition and pathology. Semin Liver Dis. 2001; 21:3–16. [PubMed: 11296695]
11. Brunt EM, Janney CG, Di Bisceglie AM, Neuschwander-Tetri BA, Bacon BR. Nonalcoholic steatohepatitis: a proposal for grading and staging the histological lesions. Am J Gastroenterol. 1999; 94:2467–2474. [PubMed: 10484010]
12. Awai HI, Newton KP, Sirlin CB, Behling C, Schwimmer JB. Evidence and Recommendations for Imaging Liver Fat in Children, Based on Systematic Review. Clin Gastroenterol Hepatol. 2014; 12:765–773. [PubMed: 24090729]
13. Tang A, Tan J, Sun M, Hamilton G, Bydder M, Wolfson T, Gamst AC, et al. Nonalcoholic fatty liver disease: MR imaging of liver proton density fat fraction to assess hepatic steatosis. Radiology. 2013; 267:422–431. [PubMed: 23382291]
14. Wu CH, Ho MC, Jeng YM, Hsu CY, Liang PC, Hu RH, Lai HS, et al. Quantification of hepatic steatosis: a comparison of the accuracy among multiple magnetic resonance techniques. J Gastroenterol Hepatol. 2014; 29:807–813. [PubMed: 24224538]
15. Permutt Z, Le TA, Peterson MR, Seki E, Brenner DA, Sirlin C, Loomba R. Correlation between liver histology and novel magnetic resonance imaging in adult patients with non-alcoholic fatty liver disease - MRI accurately quantifies hepatic steatosis in NAFLD. Aliment Pharmacol Ther. 2012; 36:22–29. [PubMed: 22554256]
16. Banerjee R, Pavlides M, Tunnicliffe EM, Piechnik SK, Sarania N, Philips R, Collier JD, et al. Multiparametric magnetic resonance for the non-invasive diagnosis of liver disease. J Hepatol. 2014; 60:69–77. [PubMed: 24036007]

17. Levenson H, Greensite F, Hoefs J, Friloux L, Applegate G, Silva E, Kanel G, et al. Fatty infiltration of the liver: quantification with phase-contrast MR imaging at 1. 5 T vs biopsy. AJR Am J Roentgenol. 1991; 156:307–312. [PubMed: 1898804]
18. Westphalen AC, Qayyum A, Yeh BM, Merriman RB, Lee JA, Lamba A, Lu Y, et al. Liver fat: effect of hepatic iron deposition on evaluation with opposed-phase MR imaging. Radiology. 2007; 242:450–455. [PubMed: 17255416]
19. Qayyum A, Chen DM, Breiman RS, Westphalen AC, Yeh BM, Jones KD, Lu Y, et al. Evaluation of diffuse liver steatosis by ultrasound, computed tomography, and magnetic resonance imaging: which modality is best? Clin Imaging. 2009; 33:110–115. [PubMed: 19237053]
20. McPherson S, Jonsson JR, Cowin GJ, O'Rourke P, Clouston AD, Volp A, Horsfall L, et al. Magnetic resonance imaging and spectroscopy accurately estimate the severity of steatosis provided the stage of fibrosis is considered. J Hepatol. 2009; 51:389–397. [PubMed: 19505740]
21. Kang BK, Yu ES, Lee SS, Lee Y, Kim N, Sirlin CB, Cho EY, et al. Hepatic fat quantification: a prospective comparison of magnetic resonance spectroscopy and analysis methods for chemical-shift gradient echo magnetic resonance imaging with histologic assessment as the reference standard. Invest Radiol. 2012; 47:368–375. [PubMed: 22543969]
22. Idilman IS, Aniktar H, Idilman R, Kabacam G, Savas B, Elhan A, Celik A, et al. Hepatic steatosis: quantification by proton density fat fraction with MR imaging versus liver biopsy. Radiology. 2013; 267:767–775. [PubMed: 23382293]
23. Qayyum A, Goh JS, Kakar S, Yeh BM, Merriman RB, Coakley FV. Accuracy of liver fat quantification at MR imaging: comparison of out-of-phase gradient-echo and fat-saturated fast spin-echo techniques--initial experience. Radiology. 2005; 237:507–511. [PubMed: 16244259]
24. Schwimmer JB. Definitive diagnosis and assessment of risk for nonalcoholic fatty liver disease in children and adolescents. Semin Liver Dis. 2007; 27:312–318. [PubMed: 17682977]
25. Kleiner DE, Brunt EM, Van Natta M, Behling C, Contos MJ, Cummings OW, Ferrell LD, et al. Design and validation of a histological scoring system for nonalcoholic fatty liver disease. Hepatology. 2005; 41:1313–1321. [PubMed: 15915461]
26. Bydder M, Yokoo T, Hamilton G, Middleton MS, Chavez AD, Schwimmer JB, Lavine JE, et al. Relaxation effects in the quantification of fat using gradient echo imaging. Magn Reson Imaging. 2008; 26:347–359. [PubMed: 18093781]
27. Liu CY, McKenzie CA, Yu H, Brittain JH, Reeder SB. Fat quantification with IDEAL gradient echo imaging: correction of bias from T(1) and noise. Magn Reson Med. 2007; 58:354–364. [PubMed: 17654578]
28. Yu H, McKenzie CA, Shimakawa A, Vu AT, Brau AC, Beatty PJ, Pineda AR, et al. Multiecho reconstruction for simultaneous water-fat decomposition and T2* estimation. J Magn Reson Imaging. 2007; 26:1153–1161. [PubMed: 17896369]
29. Yu H, Shimakawa A, McKenzie CA, Brodsky E, Brittain JH, Reeder SB. Multiecho water-fat separation and simultaneous R2* estimation with multifrequency fat spectrum modeling. Magn Reson Med. 2008; 60:1122–1134. [PubMed: 18956464]
30. Goodman LAK, William H. Measures of Association for Cross Classifications, IV: Simplification of Asymptotic Variances. Journal of the American Statistical Association. 1972; 67:415–421.
31. Schwimmer JB, Newton KP, Awai HI, Choi LJ, Garcia MA, Ellis LL, Vanderwall K, et al. Paediatric gastroenterology evaluation of overweight and obese children referred from primary care for suspected non-alcoholic fatty liver disease. Aliment Pharmacol Ther. 2013; 38:1267–1277. [PubMed: 24117728]
32. Pacifico L, Martino MD, Catalano C, Panebianco V, Bezzi M, Anania C, Chiesa C. T1-weighted dual-echo MRI for fat quantification in pediatric nonalcoholic fatty liver disease. World J Gastroenterol. 2011; 17:3012–3019. [PubMed: 21799647]
33. Deng J, Fishbein MH, Rigsby CK, Zhang G, Schoeneman SE, Donaldson JS. Quantitative MRI for hepatic fat fraction and T2* measurement in pediatric patients with non-alcoholic fatty liver disease. Pediatr Radiol. 2014
34. Hatta T, Fujinaga Y, Kadoya M, Ueda H, Murayama H, Kurozumi M, Ueda K, et al. Accurate and simple method for quantification of hepatic fat content using magnetic resonance imaging: a

prospective study in biopsy-proven nonalcoholic fatty liver disease. J Gastroenterol. 2010; 45:1263–1271. [PubMed: 20625773]

35. Lee SS, Park SH, Kim HJ, Kim SY, Kim MY, Kim DY, Suh DJ, et al. Non-invasive assessment of hepatic steatosis: prospective comparison of the accuracy of imaging examinations. J Hepatol. 2010; 52:579–585. [PubMed: 20185194]
36. Reeder SB, Cruite I, Hamilton G, Sirlin CB. Quantitative Assessment of Liver Fat with Magnetic Resonance Imaging and Spectroscopy. J Magn Reson Imaging. 2011; 34 spcone.
37. Meisamy S, Hines CD, Hamilton G, Sirlin CB, McKenzie CA, Yu H, Brittain JH, et al. Quantification of hepatic steatosis with T1-independent, T2-corrected MR imaging with spectral modeling of fat: blinded comparison with MR spectroscopy. Radiology. 2011; 258:767–775. [PubMed: 21248233]
38. Fischer MA, Nanz D, Reiner CS, Montani M, Breitenstein S, Leschka S, Alkadhi H, et al. Diagnostic performance and accuracy of 3-D spoiled gradient-dual-echo MRI with water- and fat-signal separation in liver-fat quantification: comparison to liver biopsy. Invest Radiol. 2010; 45:465–470. [PubMed: 20479652]
39. Yokoo T, Bydder M, Hamilton G, Middleton MS, Gamst AC, Wolfson T, Hassanein T, et al. Nonalcoholic fatty liver disease: diagnostic and fat-grading accuracy of low-flip-angle multiecho gradient-recalled-echo MR imaging at 1. 5 T. Radiology. 2009; 251:67–76. [PubMed: 19221054]
40. Longo R, Ricci C, Masutti F, Vidimari R, Croce LS, Bercich L, Tiribelli C, et al. Fatty infiltration of the liver. Quantification by 1H localized magnetic resonance spectroscopy and comparison with computed tomography. Invest Radiol. 1993; 28:297–302. [PubMed: 8478169]
41. Longo R, Pollesello P, Ricci C, Masutti F, Kvam BJ, Bercich L, Croce LS, et al. Proton MR spectroscopy in quantitative in vivo determination of fat content in human liver steatosis. J Magn Reson Imaging. 1995; 5:281–285. [PubMed: 7633104]
42. van Werven JR, Marsman HA, Nederveen AJ, Smits NJ, ten Kate FJ, van Gulik TM, Stoker J. Assessment of hepatic steatosis in patients undergoing liver resection: comparison of US, CT, T1-weighted dual-echo MR imaging, and point-resolved 1H MR spectroscopy. Radiology. 2010; 256:159–168. [PubMed: 20574093]
43. Szczepaniak LS, Nurenberg P, Leonard D, Browning JD, Reingold JS, Grundy S, Hobbs HH, et al. Magnetic resonance spectroscopy to measure hepatic triglyceride content: prevalence of hepatic steatosis in the general population. Am J Physiol Endocrinol Metab. 2005; 288:E462–468. [PubMed: 15339742]
44. Fishbein MH, Gardner KG, Potter CJ, Schmalbrock P, Smith MA. Introduction of fast MR imaging in the assessment of hepatic steatosis. Magn Reson Imaging. 1997; 15:287–293. [PubMed: 9201675]

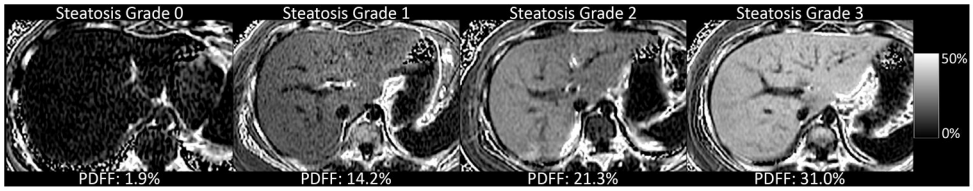

Figure 1.

Magnetic resonance imaging-estimated liver proton density fat fraction parametric maps are shown for individual children in each of the four histologically-determined steatosis grades

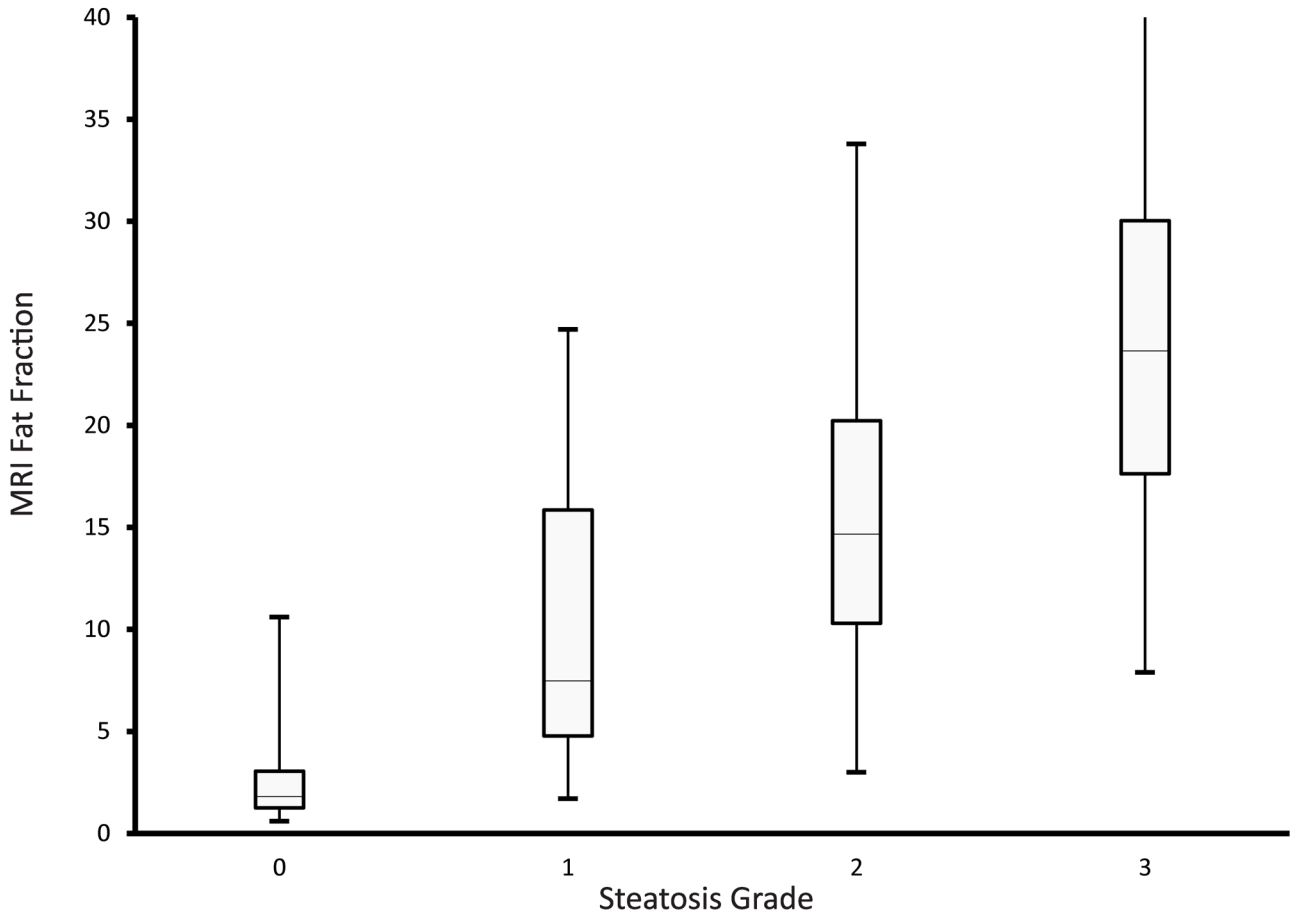

Figure 2.

Box and whiskers plot of magnetic resonance imaging-estimated liver proton density fat fraction by histologic steatosis grade. Box shows median and interquartile range, lines show minimum and maximum.

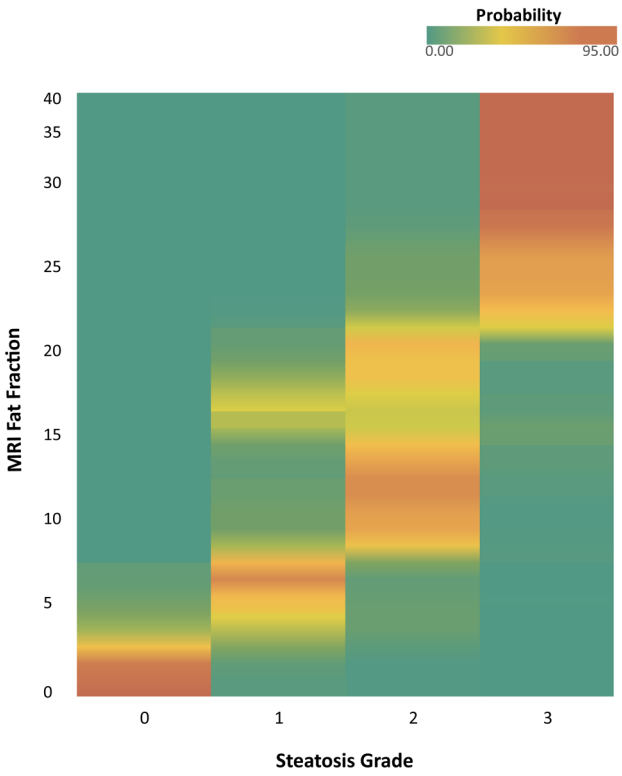

Figure 3.

Heat map shows the probability of a given magnetic resonance imaging-estimated liver proton density fat fraction corresponding to a histologic steatosis grade of 0, 1, 2, or 3.

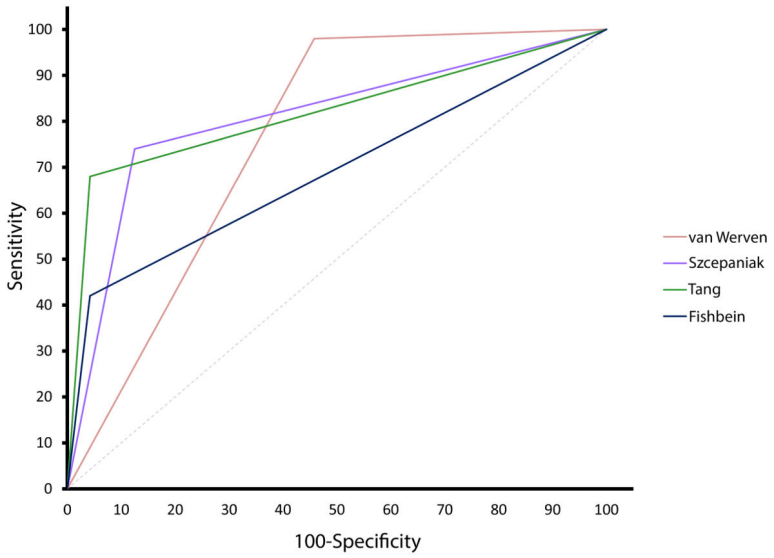

Figure 4.

Receiver operating characteristic curves for each of 4 published cutoff points to separate between histologic steatosis grades of 0 and 1.

Table 1

Characteristics of Study Population by Steatosis Grade

Variables	Grade 0 N = 24	Grade 1 N = 50	Grade 2 N = 50	Grade 3 N = 50
Age, mean (SD)	15.1 (2.5)	14.2 (2.2)	14.1 (2.2)	13.2 (2.0)
Sex, N (%)				
Boys	13 (54)	35 (70)	34 (68)	36 (72)
Girls	11 (46)	15 (30)	16 (32)	14 (28)
Weight, mean (SD), Kg	87.5 (29.8)	94.5 (21.6)	94.4 (22.8)	84.7 (20.6)
Height, mean (SD), cm**	169.2 (12.3)	164.4 (12.1)	163.4 (10.3)	160.6 (10.8)
BMI (Kg/m^2), mean (SD)	30.2 (8.3)	33.8 (6.1)	35.0 (6.6)	32.5 (5.5)
ALT, mean (SD), U/L**	22 (24)	42 (70)	44 (90)	77 (67)
AST, mean (SD), U/L**	23 (24)	33 (46)	36 (48)	49 (39)
GGT, mean (SD), U/L*	22 (15)	29 (24)	28 (45)	37 (32)
Time between biopsy and MRI, mean (SD), days	58 (11)	58 (7)	63 (7)	50 (7)
Fibrosis, N (%)**	7 (29)	21 (42)	20 (40)	27 (54)
MRI PDFF (SD)**	2.6 (2.2)	9.2 (5.8)	15.1 (6.8)	26.8 (8.2)

* $p < 0.05$;

** $p < 0.005$;

PDFF = proton density fat fraction

Table 2

Diagnostic Accuracy of Proposed Thresholds for Fatty Liver

	Author	**van Werven**	**Szczepaniak**	**Tang**	**Fishbein**
	Cut-off	**1.8%**	**5.5%**	**6.4%**	**9.0%**
Sensitivity		98	74	68	42
Specificity		54	88	96	96
AUROC		0.76	0.81	0.82	0.69